Journal of Statistical Physics, Vol. 92, Nos. 5/6, 1998

Coverage and Structure of Films of Spherical Particles Deposited after Diffusing in a Gravitational Field

Ho Suk Choi[1] and Julian Talbot[2]

Received December 2, 1998; final June 2, 1998

We investigate the coverage and structure of a layer of particles deposited on a line after diffusion in a gravitational field. The dynamics of the depositing particles is controlled by the gravity number $N_G (= \pi d^4 \Delta\rho g/6k_B T)$, where d is the diameter of the particles, $\Delta\rho$ is the density difference between the particles and the solution, g is the acceleration due to gravity, k_B is Boltzmann's constant, and T is the temperature. The position-dependent flux of particles in a gap formed by two preadsorbed particles is estimated by superposition of solutions of a steady-state convective diffusion equation for the flux in the presence of a single preadsorbed particle. The saturation coverages are found with a recursion relation and are in good agreement with those obtained from Brownian dynamics simulation. The jamming coverage increases rapidly with increasing particle size, particularly for large values of $\Delta\rho$. An algorithm is presented to generate adsorbed configurations from which the structure of the deposit is determined.

KEY WORDS: Random sequential adsorption; hard-sphere particles; gravity; diffusion; coverage; structure.

1. INTRODUCTION

The adsorption or deposition of colloidal particles (latexes, proteins, bacteria and enzymes) onto solid substrates from a bulk fluid has great importance in many different industrial fields, including chromatography, biofilters, artificial organs and biofouling.[1–3] The Langmuir equation has been widely used to quantitatively analyze the experimental results of adsorption processes. In the cases referred to above, however, each solute

[1] School of Chemical Engineering, Chungnam National University, Taejon, 305-764, Korea.
[2] Department of Chemistry and Biochemistry, Duquesne University, Pittsburgh, Pennsylvania 15282-1503.

0022-4715/98/0900-0891$15.00/0

randomly covers and bonds with many active sites on the substrate, the surface blocking effect is more complex than in the Langmuir model. The adsorption of biomacromolecules is often a random, irreversible process implying that classical equilibrium thermodynamic methods can not be directly applied.

In random sequential adsorption (RSA) particles are placed randomly and sequentially on a substrate and fixed at the initially adsorbed place if they do not overlap with preadsorbed particles. The kinetics of the model[4] and the structure of deposited particles have been studied. In particular, the saturation coverage,[5,6] $\theta_\infty = 0.547...$, is in good agreement with the experimental estimate (0.55 ± 0.01) of Onoda and Liniger[7] for the deposition of latex spheres. Although the RSA model successfully describes the random, irreversible and blocking nature of the adsorption process, it does not properly incorporate the transport mechanism of the particles from bulk to substrate. To address this issue in the case where the density difference between solute and solvent is not significant, the diffusion random sequential adsorption (DRSA) model,[8–11] based upon sequential Brownian dynamics, was developed. Many adsorption configurations are built up by a number of independent random walks from the bulk phase to the surface. Remarkably, the structure, as characterized by the radial distribution function, and the coverage of the jammed configuration generated by the DRSA model were found to be indistinguishable from those of simple RSA.[8–11]

On the other hand, when the density between solute and solvent is large, the adsorbing particles follow straight line, instead of Brownian, trajectories. To describe this situation the ballistic deposition (BD) model[12] was developed in which particles are dropped to the surface, and are accepted if they are not blocked by preadsorbed particles or if there is room near the blocking particles. In the latter case, the particles roll down the surface of the preadsorbed particles.[12–16] In BD, since the effect of nonuniform adsorption is quite significant, the kinetics and the structure of particle deposits are significantly different from those of RSA and DRSA.

In a real system, the density difference between particles and solvent may be such that the adsorption is intermediate between DRSA and BD. In addition, other factors, such as temperature and the particle size, will affect the transport mechanism of particle from bulk solution to surface. Senger *et al.*[17,18] have studied the effect of both diffusion and gravity on the adsorption of hard spheres after fixing the temperature of system and the density difference between solvent and solute, and successfully obtained the jamming coverages for particles with different sizes. However, the sequential Brownian dynamics simulation which they used has several drawbacks, including the expense and the uncertainty which results from

the use of a finite mesh and the starting point of the diffusing particles. Recently, Faraudo and Bafaluy[19] have developed an approximate general formalism and showed that the saturation coverage approaches the ballistic limit following a power law in N_G, the gravity number(defined later), which is independent of the number of dimensions. In our previous paper,[20] we have solved a steady state convective-diffusion equation using a collocation method to find the concentration profile and the particle flux distribution in the presence of a single preadsorbed particle on a line.

Here, we extend the work to the calculation of the saturation coverages and the radial distribution function of particle deposits. We describe theoretical and numerical details in the following section. We develop a fitting function which enables us to analyze quantitatively the saturated structures formed by deposition of particles on one-dimensional surfaces under the influence of both gravity and brownian forces. Finally, we attempt to explain qualitatively experimental observations of large particles adhering on flat silica surfaces (2-dimensional). We do not take into account the effect of hydrodynamic interactions and colloidal forces on the deposition process.[21]

2. THEORY

A simple model has been developed to understand the structure of the adsorbed layer of particles under two simple transport mechanisms, namely, diffusion and sedimentation.[19,20] Figure 1 illustrates the deposition of a third particle in the presence of two preadsorbed particles. An adsorbing line is at $y=0$ and a semi-infinite fluid is in the region $y>0$. Spherical particles of diameter, d, suspended in the fluid diffuse in the xy-plane and sediment due to the effect of gravity in the y-direction. If the center of a new particle arrives at the $y=0$ line, it is adsorbed irreversibly at the contact point. The surfaces of the preadsorbed particles act as reflecting boundaries. Thus, at large values of the gravity number particles arriving on top of preadsorbed particles tend to roll down over them to the adsorbing line. It is assumed that the concentration of particles is so small that interactions between them are negligible in the bulk. Consequently, each particle adsorbs independently of the other particles in the suspension, and the process can be regarded as sequential. However, the concentration becomes large at the surface, where adsorbed particles accumulate and interact via excluded volume effects with incoming particles.

This adsorption problem can be solved in three steps: first, the transport equation for a single particle near the surface is solved in the presence of a single preadsorbed particle; second, this solution is used to calculate approximately the adsorption probability in the presence of two preadsorbed

particles; finally, this adsorption probability allows us to generate configurations of adsorbed particles from which the structure of the adsorbed layer can be determined.

The governing transport equation is written to obtain the rate of arrival of an adsorbing particle near a preadsorbed particle in a 1 + 1 D system:[20–23]

$$\frac{\partial^2\psi}{\partial r^2}+\left(\frac{1}{r}+N_G\sin\theta\right)\frac{\partial\psi}{\partial r}+\frac{1}{r^2}\frac{\partial^2\psi}{\partial\theta^2}+N_G\frac{\cos\theta}{r}\frac{\partial\psi}{\partial\theta}=0 \tag{1}$$

where ψ is the normalized concentration distribution (probability function) of particles in solution phase:

$$\psi=\frac{c}{c_0} \tag{2}$$

and N_G is the dimensionless gravity number:

$$N_G=\frac{\pi d^4\,\Delta\rho g}{6k_{\mathrm{B}}T} \tag{3}$$

where $\Delta\rho$ is the density difference between the particle and the solution, g is the acceleration due to gravity, k_{B} is Boltzmann's constant and T is temperature. The boundary conditions $\psi=0$ are at $y=0$ (adsorbing), $\partial\psi/\partial r+N_G\sin\theta\psi=0$ (reflecting boundary at the surface of the preadsorbed sphere) and $\partial\psi/\partial\theta=0$ at $\theta=\pi/2$ (symmetry). Full details are presented in the Appendix.

The solution of the transport equation is obtained numerically with a collocation method and formulated as fitting functions in the previous paper.[20] Differentiating the probability function results in the flux of particles at the solid-liquid interface:

$$J(x)|_{y=0}=-D\left(\frac{\partial c}{\partial y}\right)_{y=0}=-Dc_0\left(\frac{\partial\psi}{\partial y}\right)_{y=0} \tag{4}$$

where x is the position on the surface relative to the center of the preadsorbed particle. After dividing ψ into two parts, ψ_0 and ψ_1, and substituting them into Eq. (4), one has the following equation:

$$J(x)=J_0+J_1(x) \tag{5}$$

where

$$J_0=-Dc_0N_G \tag{6}$$

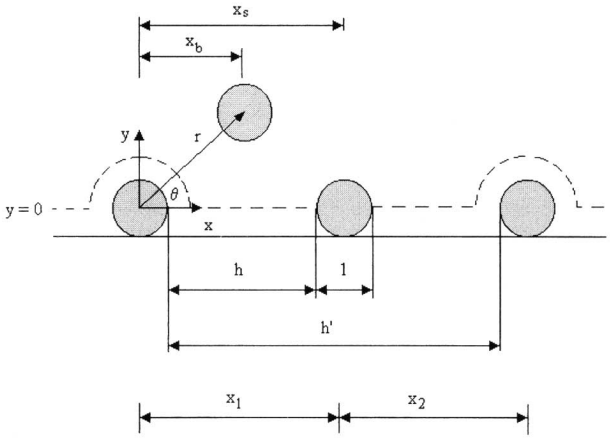

Fig. 1. Illustration of the adsorption process. A disk is inserted in a gap of length h' to produce two smaller gaps of length h and $h'-h-1$.

is the flux on an empty surface and J_1, therefore, shows the effects of lateral diffusion relative to convection due to gravity in the presence of one preadsorbed particle. $J_1 = 0$ in the absence of a preadsorbed particle and J_1 tends to zero sufficiently far from a preadsorbed particle.

We now consider the deposition of a particle in a gap of width h' formed by two previously deposited particles. See Fig. 1. As a first approximation, the deviations of the flux from its value on a bare surface, J_0, induced by each preadsorbed particle are independent and can be added:

$$J(x_1, x_2) \approx J_0 + J_1(x_1) + J_1(x_2) \tag{7}$$

where x_1 and x_2 are the distances from the centers of each preadsorbed particle and are related to the gap widths as $x_1 = h + 1$ and $x_2 = h' - h$ (Fig. 1).

We now introduce $P(h', h)$ to denote the probability that insertion of a particle into a gap of size h' produces gaps of width h and $h'-h-1$. Clearly,

$$P(h', h) \propto J(x_1, x_2) \tag{8}$$

and imposing the normalization condition

$$\int_0^{h'-1} P(h', h)\, dh = 1 \tag{9}$$

yields

$$P(h',h)=\frac{1}{A(h')}\,(1+f(h+1)+f(h'-h)) \tag{10}$$

where $f(x)=J_1(x)/J_0$ and $A(h')=h'-1+2F(h')$ with $F(h')=\int_1^{h'} f(x)\,dx$.

In the previous paper[20] it was found that an accurate fit of the numerical solution of the convective-diffusion equation is provided by the emperical function:

$$\frac{J_1(x)}{J_0}=\sum_{i=1}^{6}\frac{\gamma_i}{x^{2i}} \tag{11}$$

where γ_i are the fitting coefficients. The probability was determined by substituting (11) into (10).

One may use the following recursive formula to calculate the average number of particles that are in the gap at length h' after an infinite time, $N_\infty(h')$:

$$N_\infty(h')=1+2\int_0^{h'-1} N_\infty(h)\,P(h',h)\,dh \tag{12}$$

with the initial solutions:

$$N_\infty^{(1)}(h')=0, \qquad 0\leqslant h'<1 \tag{13}$$

$$N_\infty^{(2)}(h')=1, \qquad 1\leqslant h'<2 \tag{14}$$

Now, the mean saturation coverage of particles adsorbed in a confined gap of length h' is

$$\theta_\infty(h')=\frac{N_\infty(h')}{h'} \tag{15}$$

From Renyi's original work,[24] one has the following asymptotic relation:

$$\theta_\infty(\infty)-\theta_\infty(h')\sim\frac{1}{h'} \tag{16}$$

Using the above procedure, one can only approximately calculate the saturation coverages of particle deposits, since we apply a superposition hypothesis to obtain Eq. (9) and do not take into account the effect of additional preadsorbed particles which result in an asymmetric adsorption probability.[20] These two factors, however, only slightly affect the value of saturation coverages.[20]

An estimate of the saturation coverage at a given value of N_G may be obtained directly from $P(h',h)$ and the recursive relation, (12). To determine the structure of the adsorbed layer, however, it is necessary to simulate the process to obtain actual configurations of particles from which the radial distribution function may be determined.

Particles are added to a given configuration as follows. Let $\{x_i, i = 0,..., N+1\}$ specify a given configuration with $x_0 = -1$ and $x_{N+1} = L+1$ (particles 0 and $N+1$ are initially fixed in these positions to form a gap of length $L+1$). The available line for insertion of a new particle is

$$L_0 = \sum_{i=0}^{N} \max(x_{i+1} - x_i - 2, 0) \tag{17}$$

We add a new particle to the configuration by first selecting a gap in which to place it. Let $z = \xi_1 L_0$ where $0 < \xi_1 < 1$ is a uniform random number. This corresponds to the gap between particles j and $j+1$ where

$$\sum_{i=0}^{j-1} \max(x_{i+1} - x_i - 2, 0) < \xi_1 L_0 < \sum_{i=0}^{j} \max(x_{i+1} - x_i - 2, 0) \tag{18}$$

The next step is to place the particle in the selected gap of length h' with a probability $P(h', h)$. This is achieved by generating another uniform random number ξ_2 and solving numerically the following for h:

$$\int_0^h P(h', h)\, dh = \xi_2 \tag{19}$$

where the integral is the cumulative probability that the adsorbed particle lies in the interval $(0, h)$. For example, if $\xi_2 = 0, h = 0$; if $\xi_2 = 1, h = h' - 1$. The particle is placed at position h and the process can be continued until all gaps are smaller than the particle diameter and the configuration is jammed. Note that with this algorithm, there are no rejected attempts: a particle is always placed into an available gap.

One may use the following approximate form of $P(h', h)$ suggested by Faraudo and Bafaluy.[19]

$$P(h',h) = \frac{1 + be^{-bh} + be^{-b(h'-h-1)}}{h' + 1 - 2e^{-b(h'-1)}} \tag{20}$$

where

$$b = \frac{N_G^{2/3}}{\alpha}, \quad \alpha = 1.08... \tag{21}$$

3. RESULTS AND DISCUSSION

3.1. Adsorption Probability Distribution

We obtain the approximate probability distribution of particles adsorbing between two preadsorbed particles at different N_G values in a gap of size $h' = 4$, as shown in Fig 2. To obtain these probability distributions, we use Eqs. (9) and (10). The probability distribution at $N_G = 1.0$ is almost identical to that of the pure diffusional case with a relatively uniform distribution of particles. As N_G increases, the probability of adsorption in the vicinity of two preadsorbed particles increase tremendously, while that in the middle of the gap approaches a constant value. This is because as N_G increases, the deterministic motion of particles due to gravity becomes more important than the random brownian motion. For large values of N_G, $P(h', h)$ contains a singular contribution from two delta functions at each side of the gap plus a constant in the middle of the gap. Finally, when $N_G = \infty$, the adsorption process becomes ballistic deposition.[12]

3.2. Saturation Coverage

Using $P(h',h)$ and Eqs. (12)–(16), one can determine the saturation coverage of the process. The basic idea of the recursion formula, Eq. (12), is that, in the irreversible adsorption of disks on a confined line segment of

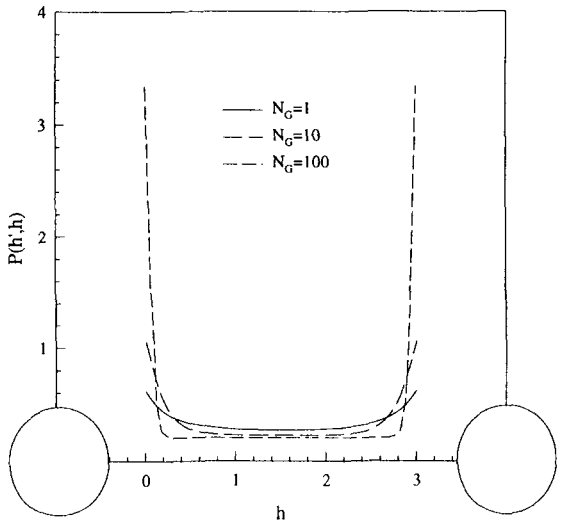

Fig. 2. Comparison of probability distribution functions, $P(h',h)$ calculated at different values of N_G for $h' = 4$.

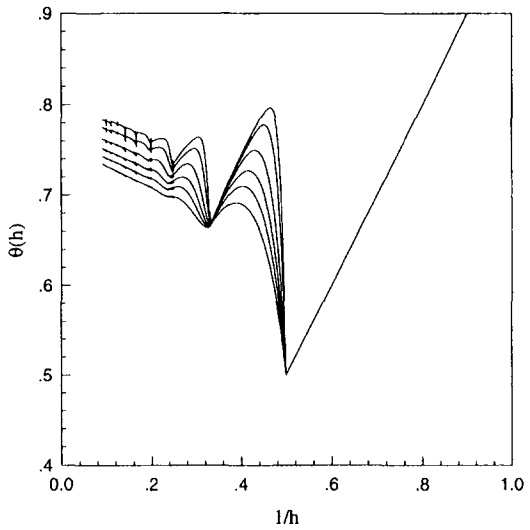

Fig. 3. Asymptotic behavior of the mean saturation coverages of particles deposited in a gap of size h, $\theta_\infty(h)$, at different gravity numvers: $N_G = 1, 5, 10, 20, 50, 100$ from bottom to top, respectively.

length, h', one can determine the average number of spherical particles that are in the gap after an infinite time, since the insertion of one particle into a gap produces two additional small gaps. Figure 3 shows a linear relation between the mean saturation coverage of particles adsorbed in a confined gap of size h, $\theta_\infty(h)$, and the inverse of gap size, $1/h$, when h is greater than about 5. From the intersection of the extrapolation with the line $1/h = 0$, one can obtain the saturation coverage at each value of N_G. This method is remarkably accurate and fast compared with other methods like brownian dynamics simulation.

Figure 4 shows the variation of the saturation coverage with the gravity number. As expected, the saturation coverage increases monotonically as N_G increases and approaches the maximum coverage of the BD process. When $N_G = 1.0$, the saturation coverage is almost the same as that of DRSA process. Although the saturation coverages in this study are obtained with an approximate superposition principle, they are indistinguishable from those obtained using the more time consuming method of brownian dynamics simulation.

Faraudo and Bafaluy[19] found an asymptotic expression for the saturation coverages as a function of N_G, which is accurate in the strong gravity limit, $N_G \to \infty$:

$$\theta_\infty(N_G \gg 1) \cong \theta_\infty^{\mathrm{BD}} - 0.2445 N_G^{-2/3} \tag{22}$$

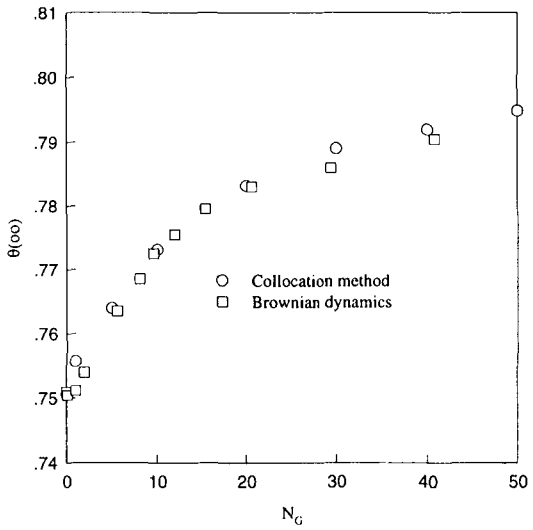

Fig. 4. Comparison of saturation coverages calculated in this study (empty circles) with the Brownian dynamics results (empty squares).

where $\theta_\infty^{BD} = 0.80865$ is the jamming limit of BD model. Using this expression and the numerical data obtained from the simulation, we developed the following semi-empirical equation:

$$\frac{\theta_\infty^{\mathrm{BD}} - \theta_\infty(N_G)}{\theta_\infty^{\mathrm{BD}} - \theta_\infty^{\mathrm{DRSA}}} = \frac{1 + a_1 N_G^2 + N_G^3}{1 + a_2 N_G^2 + a_3 N_G^3 + a_4 N_G^{11/3}} \tag{23}$$

where $a_1 = 1.767, a_2 = 2.262, a_3 = 0.620, a_4 = 0.237$ and $\theta_\infty^{\mathrm{DRSA}}$ is the saturation coverage of DRSA model, 0.7506. This equation has the correct asymptotic behavior but, otherwise, its form is arbitrary. To obtain the above fitting function, Eq. (23), we first fixed the coefficient, $a_4 = (\theta_\infty^{\mathrm{BD}} - \theta_\infty^{\mathrm{DRSA}})/0.2445 = 0.237...$ and then simultaneously adjusted the other 3 parameters to obtain the best least squares fit of the simulation data. As shown in Fig. 5, the fitting function agrees very well with simulation data. We now consider the effect of particle size on the structure of saturated particle deposits. We define a dimensionless diameter,

$$d^* \equiv \frac{d_p}{(6kT/\pi \Delta\rho g)^{1/4}} = \frac{d_p}{l_c} = N_G^{1/4} \tag{24}$$

where l_c is a characteristic length which depends on the temperature and the density difference between fluid and particle. Using this relation, we replot Fig. 5 as a function of d_p for different values of $\Delta\rho$ (or T). Figure 6

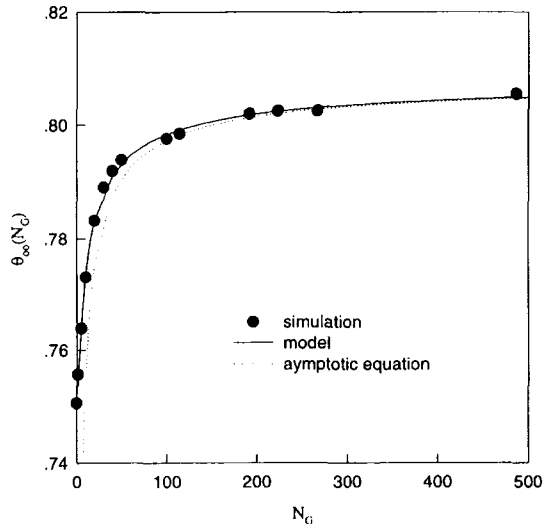

Fig. 5. Rational fitting function, Eq. (20), for the saturation coverage as a function of N_G, which is in good agbreement with both the numerical simulation results and the asymptotic equation, Eq. (19).

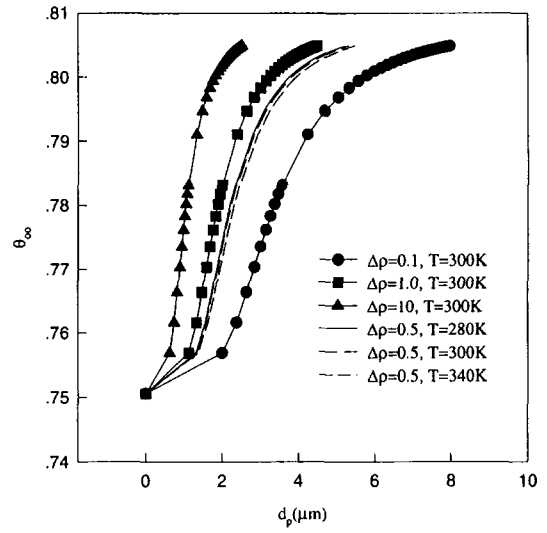

Fig. 6. Effect of particle size on the saturation coverages calculated at various values of $\Delta\rho$ and T.

shows that the jamming coverage increases dramatically with small increases in particle size, especially when $\Delta\rho$ is very large ($\geqslant 10$ g/cm^3). When $\Delta\rho = 0.1$ g/cm^3 (relatively small), the saturation coverage changes gradually from the DRSA limit to the BD limit over a wider range of particle sizes, $2 < d_p < 6$. Unlike the density difference, temperature does not strongly affect the deposition process. Figure 6 can also be regarded as a 1-dimensional equation of state:

$$\theta_\infty = \theta_\infty(d_p, \Delta\rho, T) \tag{25}$$

Thus, when any two of the independent parameters are fixed, one can deduce the effect of the remaining unfixed parameter on the saturation coverage. Among the three parameters, particle size is a major factor determining the dynamics of particles in the bulk fluid and, subsequently, the saturated structure of particle deposits on the surface. The density difference for a certain range of particle sizes also has a strong effect. For example, at $d_p = 2\mu$m, for an increase of $\Delta\rho$ from 0.1 to 1 g/cm^3, the saturation coverage increases from 0.755 to 0.79.

3.3. Structure of the First Layer of Particle Deposits

Using the method outlined in Section 2, one can obtain the structure of the adsorbed layer of particles for different values of N_G. When N_G is very large, a particle coming down onto a preadsorbed particle is fixed near the preadsorbed particle but, when N_G is small, the particle coming down onto a preadsorbed particle lands, on average, farther from the preadsorbed particle. The radial distribution function, $g(r)$, was calculated from the stored positions of adsorbed particles. This function quantifies the effect of different transport mechanisms on the structure of particle deposits. In Fig. 7, we compare 4 different saturated structures of particle deposits corresponding to $N_G = 1$, 10, 20, 50. As N_G increases, peaks of $g(r)$ at $r = 1$ and near $r = 2$ increase and become sharp. This is because the effect of diffusion due to the collision of small fluid molecules becomes weaker than that of convection due to gravity when the particle is large. Although peaks of $g(r)$ at $r = 1$ sharpen with increasing N_G, δ-function singularities do not appear even at large value of N_G (e.g., $N_G = 50$). Wojtaszczyk *et al.*[25] obtained the structure of melamine formaldehyde particles of approximate diameter 4.46 μm and density 1.5 g/cm^3 deposited from aqueous solution at room temperature (T = 300K). In this case, the dimensionless gravity number is approximately 245. For these experimental conditions and from Fig. 6, it is apparent that the saturation coverage of the experiment is near the BD limit.

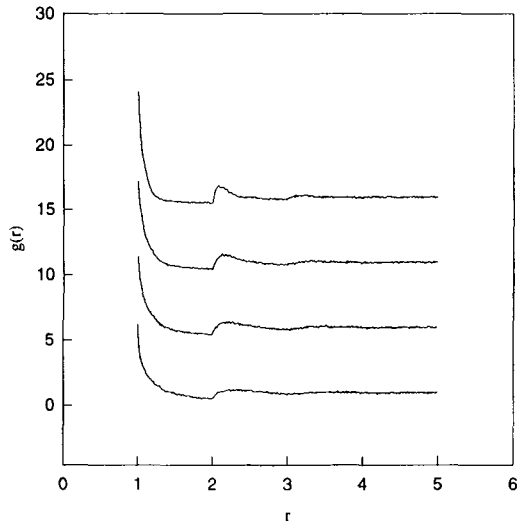

Fig. 7. Comparison of the radial distribution functions (jamming limit) calculated at different values of N_G: $N_G = 1, 10, 20, 50$, bottom to top. Successive plots are offset by 5 units for clarity.

4. CONCLUSION

We have used solutions of a steady-state convective diffusion equation to calculate the saturation coverages of particles for different values of N_G. To complete the calculation of jamming coverages, we first obtained an approximate probability distribution function, $P(h', h)$ which is proportional to the flux of incoming particles between two preadsorbed particles forming a gap of size h. As N_G increases, the function approaches two delta functions near two preadsorbed particles plus a constant contribution in the middle of the gap. Inserting $P(h', h)$ into a recursive formula, Eq. (12), yields the saturation coverage in a confined gap of size h, $\theta(h)$, as shown in Fig. 3. Extrapolating $\theta(h)$ to $1/h = 0$, the saturation coverages are obtained and they are in good agreement with the numerical results obtained from brownian dynamics simulation. A semi-empirical fitting function, Eq. (23), enables us to predict the saturation coverage and the structure of particle deposits. Using this fitting function, we investigated the effect of particle size, density difference and temperature on the deposition process. As shown in Fig. 6, the particle size is a major factor in determining the structure of particle deposits, but the density difference can also be an important factor. Finally, we developed an algorithm to generate

configurations from which the radial distribution function, $g(r)$ was determined. $g(r)$ shows more solid-like structure as N_G increases.

APPENDIX. APPLICATION OF THE COLLOCATION METHOD

To solve Eq. (2), we used a collocation method. For the sake of convenience, we transformed the convective-diffusion equation from (r, θ)-coordinates to normalized $(\tilde{r}, \tilde{\theta})$-coordinates in $1+1$ and $2+1$ D systems:

$$\tilde{\theta} = \frac{2}{\pi}\theta, \qquad \tilde{r} = \frac{r-1}{r_0 - 1} \tag{A.1}$$

Now, the convective-diffusion equation can be written as

$$\frac{\partial^2 \psi}{\partial \tilde{r}^2} + f(\tilde{r}, \tilde{\theta}) \frac{\partial \psi}{\partial \tilde{r}} + g(\tilde{r}) \frac{\partial^2 \psi}{\partial \tilde{\theta}^2} + h(\tilde{r}, \tilde{\theta}) \frac{\partial \psi}{\partial \tilde{\theta}} = 0 \tag{A.2}$$

and, in the $1+1$ D system,

$$f(\tilde{r}, \tilde{\theta}) = \left[\frac{1}{k+\tilde{r}} + \frac{N_G}{k} \sin\left(\frac{\pi}{2}\tilde{\theta}\right) \right] \tag{A.3}$$

$$g(\tilde{r}, \tilde{\theta}) = \frac{1}{(k+\tilde{r})^2} \left(\frac{2}{\pi}\right)^2 \tag{A.4}$$

$$h(\tilde{r}, \tilde{\theta}) = \frac{N_G}{k(k+\tilde{r})} \cos\left(\frac{\pi}{2}\tilde{\theta}\right) \left(\frac{2}{\pi}\right) \tag{A.5}$$

where

$$k = \frac{1}{r_0 - 1} \tag{A.6}$$

and, in the $2+1$ D system,

$$f(\tilde{r}, \tilde{\theta}) = \left[\frac{2}{k+\tilde{r}} + \frac{N_G}{k} \sin\left(\frac{\pi}{2}\tilde{\theta}\right) \right] \tag{A.7}$$

$$h(\tilde{r}, \tilde{\theta}) = -\left[\frac{\tan((\pi/2)\tilde{\theta})}{(k+\tilde{r})^2} - \frac{N_G}{k(k+\tilde{r})} \cos\left(\frac{\pi}{2}\tilde{\theta}\right) \right] \left(\frac{2}{\pi}\right) \tag{A.8}$$

respectively, with the boundary conditions (in both 1D and 2D)

$$\begin{aligned}
&\frac{\partial \psi}{\partial \tilde{r}} = -\frac{N_G}{k}\sin\left(\frac{\pi}{2}\tilde{\theta}\right)\psi && \text{at } \tilde{r}=0 \text{ and } 0\leqslant\tilde{\theta}\leqslant 1\\
&\psi = 1-\exp\left[-N_G r_0 \sin\left(\frac{\pi}{2}\tilde{\theta}\right)\right] && \text{at } \tilde{r}=1 \text{ and } 0\leqslant\tilde{\theta}\leqslant 1\\
&\psi = 0 && \text{at } \tilde{\theta}=0 \text{ and } 0\leqslant\tilde{r}\leqslant 1\\
&\frac{\partial \psi}{\partial \tilde{\theta}} = 0 && \text{at } \tilde{\theta}=1 \text{ and } 0\leqslant\tilde{r}\leqslant 1
\end{aligned} \tag{A.9}$$

The approximate solution of the above diffusion equation can be written as a linear combination of Lagrangian Polynomials such as

$$\psi(\tilde{r},\tilde{\theta}) = \sum_{j=1}^{m+2} l_j(\tilde{\theta}) \sum_{i=1}^{n+2} l_i(\tilde{r})\,\psi_{ij} \tag{A.10}$$

where

$$l_i(\tilde{r}) = \prod_{k=1,\,k\neq i}^{n} \frac{\tilde{r}-\tilde{r}_k}{\tilde{r}_i-\tilde{r}_k} \tag{A.11}$$

and

$$l_j(\tilde{\theta}) = \prod_{k=1,\,k\neq j}^{m} \frac{\tilde{\theta}-\tilde{\theta}_k}{\tilde{\theta}_j-\tilde{\theta}_k} \tag{A.12}$$

where n and m are the number of collocation points in r-direction and θ-direction, respectively. Let us denote

$$\begin{aligned}
l_j(\tilde{r}_i) &= L_{ij}, & l_j(\tilde{\theta}_i) &= L'_{ij}\\
\frac{\partial l_j(\tilde{r}_i)}{\partial \tilde{r}} &= A_{ij}, & \frac{\partial l_j(\tilde{\theta}_i)}{\partial \tilde{\theta}} &= A'_{ij}\\
\frac{\partial^2 l_j(\tilde{r}_i)}{\partial \tilde{r}^2} &= B_{ij}, & \frac{\partial^2 l_j(\tilde{\theta}_i)}{\partial \tilde{\theta}^2} &= B'_{ij}
\end{aligned} \tag{A.13}$$

Since the Lagrangian polynomial has the following property:

$$L_{ij} = \begin{cases} 0, & \text{if } i\neq j \\ 1, & \text{if } i=j \end{cases} \tag{A.14}$$

we can replace the partial derivatives of Eq. (A.2) with linear combinations of Lagrangian polynomials:

$$\psi(\tilde{r}_k, \tilde{\theta}_l) = \sum_{j=1}^{m+2} \sum_{i=1}^{n+2} L'_{lj} L_{ki} \psi_{ij} = \psi_{kl} \tag{A.15}$$

$$\frac{\partial \psi(\tilde{r}_k, \tilde{\theta}_l)}{\partial \tilde{r}} = \sum_{j=1}^{m+2} \sum_{i=1}^{n+2} L'_{lj} A_{ki} \psi_{ij} = \sum_{i=1}^{n+2} A_{ki} \psi_{il} \tag{A.16}$$

$$\frac{\partial^2 \psi(\tilde{r}_k, \tilde{\theta}_l)}{\partial \tilde{r}^2} = \sum_{i=1}^{n+2} B_{ki} \psi_{il} \tag{A.17}$$

$$\frac{\partial \psi(\tilde{r}_k, \tilde{\theta}_l)}{\partial \tilde{\theta}} = \sum_{j=1}^{m+2} A'_{lj} \psi_{kj} \tag{A.18}$$

$$\frac{\partial^2 \psi(\tilde{r}_k, \tilde{\theta}_l)}{\partial \tilde{\theta}^2} = \sum_{j=1}^{m+2} B'_{lj} \psi_{kj} \tag{A.19}$$

Substituting Eqs. (A.15)–(A.19) into Eq. (A.2), we can construct the residual function $R(\tilde{r}, \tilde{\theta})$:

$$\begin{aligned} R(\tilde{r}_k, \tilde{\theta}_l) = & \sum_{i=1}^{n+2} [B_{ki} \psi_{il} + f(\tilde{r}_k, \tilde{\theta}_l) A_{ki} \psi_{il}] \\ & + \sum_{j=1}^{m+2} [g(\tilde{r}_k) B'_{lj} \psi_{kj} + h(\tilde{r}_k, \tilde{\theta}_l) A'_{lj} \psi_{kj}] \end{aligned} \tag{A.20}$$

And the boundary conditions can be written as follows:

$$\begin{aligned} & \frac{\partial \psi(\tilde{r}_1, \tilde{\theta}_l)}{\partial \tilde{r}} + \frac{N_G}{r} \sin\left(\frac{\pi}{2} \tilde{\theta}_l\right) \psi = \sum_{i=1}^{n+2} A_{1i} \psi_{il} + \frac{N_G}{k} \sin\left(\frac{\pi}{2} \tilde{\theta}_l\right) \psi_{1l} = 0 \\ & \psi(\tilde{r}_{h+2}, \tilde{\theta}_l) = 1 - \exp\left[-N_G r_0 \sin\left(\frac{\pi}{2} \tilde{\theta}_l\right)\right] \\ & \psi(\tilde{r}_k, \tilde{\theta}_l) = 0 \\ & \frac{\partial \psi(\tilde{r}_k, \tilde{\theta}_l)}{\partial \tilde{\theta}} = \sum_{j=1}^{m+2} A'_{n+2,j} \psi_{kj} = 0 \end{aligned} \tag{A.21}$$

After inserting the boundary conditions Eq. (A.21) into Eq. (A20) and rearranging it, we finally obtain the following algebraic equation:

$$R(\tilde{r}_k, \tilde{\theta}_l) = \sum_{i=2}^{n+1} \left[B_{ki} - B_{k1} \frac{A_{1i}}{\alpha_{11}} + f(\tilde{r}_k, \tilde{\theta}_l) \left(A_{ki} - A_{k1} \frac{A_{1i}}{\alpha_{11}} \right) \right] \psi_{il} + \sum_{j=2}^{m+1} \left[g(\tilde{r}_k) \left(B'_{lj} - B'_{l,m+2} \frac{A'_{m+2,j}}{A'_{m+2,m+2}} \right) \right] + \sum_{j=2}^{m+1} \left[h(\tilde{r}_k, \tilde{\theta}_l) \left(A'_{lj} - A'_{l,m+2} \frac{A'_{m+2,j}}{A'_{m+2,m+2}} \right) \right] + D(\tilde{r}_k, \tilde{\theta}_l) \quad \text{(A.22)}$$

where

$$D(\tilde{r}_k, \tilde{\theta}_l) = \left[\left(B_{k,n+2} - B_{k1} \frac{A_{1,n+2}}{\alpha_{11}} \right) + f(\tilde{r}_k, \tilde{\theta}_l) \left(A_{k,n+2} - A_{k1} \frac{A_{1,n+2}}{\alpha_{11}} \right) \right] \times \left[r_0 \sin\left(\frac{\pi}{2} \tilde{\theta}_l \right) \right] \quad \text{(A.23)}$$

$$\alpha_{11} = A_{11} + \frac{N_G}{k} \sin\left(\frac{\pi}{2} \tilde{\theta}_l \right) \quad \text{(A.24)}$$

ACKNOWLEDGMENTS

The work reported here was supported by KOSEF Grant No. 971-1105-032-2.

REFERENCES

1. J. D. Andrade, and V. Hlady, *Adv. Polymer Sci.* **79**:1 (1987).
2. J. D. Andrade, *Surface and Interfacial Aspects of Biomolecular Polymers*, J. D. Andrade, ed., Vol. 2, Protein Adsorption (Plenum Press, New York, 1985).
3. J. D. Andrade, *Thin Solid Films* **152**:335 (1987).
4. P. Schaaf and J. Talbot, *Phys. Rev. Lett.* **62**:175 (1989).
5. J. Feder, *J. Theor. Biol.* **87**:237 (1980).
6. E. L. Hinrichsen, J. Feder, and T. Jøssang, *J. Stat. Phys.* **44**:793 (1986).
7. G. Y. Onoda and B. G. Liniger, *Phys. Rev. Lett.* **73**:114 (1986).
8. B. Senger, J.-C. Voegel, P. Schaaf, A. Johner, A. Schmitt, and J. Talbot, *Phys. Rev. A* **44**:6926 (1991).
9. B. Senger, P. Schaaf, J.-C. Voegel, A. Johner, A. Schmitt, and J. Talbot, *J. Chem. Phys.* **97**:3813 (1992).
10. B. Senger, J. Talbot, P. Schaaf, A. Schmitt, and J.-C. Voegel, *Europhys. Lett.* **21**:135 (1993).
11. F. J. Bafaluy, H. S. Choi, B. Senger, and J. Talbot, *Phys. Rev. E* **51**:5985 (1995).
12. J. Talbot and S. Ricci, *Phys. Rev. Lett.* **68**:958 (1992).

13. R. Jullien and P. Meakin, *J. Phys. A.* **25**:L189 (1992).
14. A. P. Thompson and E. D. Glandt, *Phys. Rev. A* **46**:4639 (1992).
15. H. S. Choi, J. Talbot, G. Tarjus, and P. Viot, *J. Chem. Phys.* **99**:9296 (1993).
16. H. S. Choi, Ph.D. diss., Purdue University, West Lafayette, IN, USA (1995).
17. B. Senger, F. J. Bafaluy, P. Schaaf, A. Schmitt, and J.-C. Voegel, *Proc. Nat. Acad. Sci.* **89**:9449 (1992).
18. B. Senger, R. Ezzeddin, F. J. Bafaluy, P. Schaaf, F. J. G. Cuisinier, and J.-C. Voegel, *J. Theor. Biol.* **163**:457 (1993).
19. J. Faraudo and J. Bafaluy, *Phys. Rev. E* **54**:3725 (1996).
20. H. S. Choi and J. Talbot, *Korean J. of Chem. Eng.* **14**:117 (1997).
21. J. Pagonabaraga and J. M. Rub, *Phys. Rev. Lett.* **73**:114 (1994).
22. M. Elimelech, *J. Colloid Interface Sci.* **164**:190 (1994a).
23. M. Elimelech, *Sep. Technol.* **4**:186 (1994b).
24. A. Renyi, *Publ. Math. Inst. Hung. Acad. Sci.* **3**:109, (1958).
25. P. Wojtaszczyk, P. Schaaf, B. Senger, M. Zembala, and J. C. Voegel, *J. Chem. Phys.* **99**:7198 (1993).